Macromolecules

Article

pubs.acs.org/Macromolecules

Onset of Non-Continuum Effects in Microrheology of Entangled Polymer Solutions

Cole D. Chapman,[‡] Kent Lee,[†] Dean Henze,[†] Douglas E. Smith,[‡] and Rae M. Robertson-Anderson*[,†]

[†]Department of Physics, University of San Diego, San Diego, California 92110, United States

[‡]Department of Physics, University of California San Diego, La Jolla, California 92093, United States

ABSTRACT: Microrheology has emerged as a powerful approach for elucidating mechanical properties of soft materials and complex fluids, especially biomaterials. In this technique, embedded microspheres are used to determine viscoelastic properties via generalized Stokes−Einstein relations, which assume the material behaves as a homogeneous continuum on the length scale of the probe. However, this condition can be violated if macromolecular systems form characteristic length scales that are larger than the probe size. Here we report observations of the onset of this effect in DNA solutions. We use microspheres driven with optical tweezers to determine the frequency dependence of the linear elastic and viscous moduli and their dependence on probe radius and DNA length. For well-entangled DNA, we find that the threshold probe radius yielding continuum behavior is ∼3× the reptation tube diameter, consistent with recent theoretical predictions. Notably, this threshold is significantly larger than the mesh size of the polymer network, and larger than typical probe sizes used in microrheology studies.

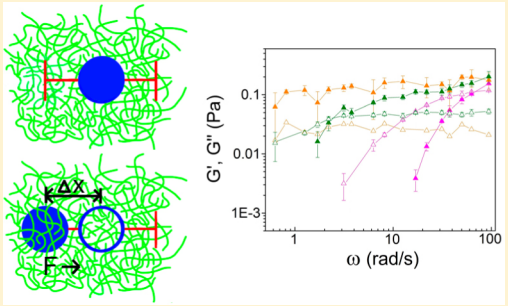

INTRODUCTION

Polymeric fluids and soft matter, ubiquitous in nature and industry alike, display complex and intriguing mechanical properties. As such, numerous studies have been devoted to understanding their stress−strain relationships;[1−4] however, many unanswered questions remain. In standard rheology studies, macroscopic strains are applied and bulk-induced stress is measured to quantify the frequency dependence of elastic and viscous responses. In contrast, microrheology uses embedded microspheres, either diffusing passively or driven by magnetic or optical tweezers, to probe mechanical properties at the microscale.[5−18] Microrheology has emerged as a powerful complementary approach to standard macrorheology and has many advantages, including small sample sizes, small applied strains (important for fragile biomaterials), and the ability to detect microscale heterogeneities and fluctuations.[18,19]

In microrheology studies, measurements of microsphere motion are interpreted to deduce viscoelastic moduli via generalized Stokes−Einstein relations.[15] Theoretically, such an analysis should yield accurate determinations of macroscopic material properties provided the material behaves as a near-equilibrium, homogeneous, isotropic continuum on the size scale of the probing microsphere. It is widely accepted that when polymers overlap to form a transient mesh the embedded probe should be chosen to be larger than the characteristic mesh size to access macroscopic rheological properties. Alternatively, probes smaller than the mesh size can and have been used to determine microscale structures and heterogeneities present in polymer systems.[16−18] Several recent experiments have employed passive nanoparticle tracking to examine both microscale and macroscale properties of flexible synthetic polymers, such as poly(ethylene oxide) (PEO), poly(ethylene glycol) (PEG), and polystyrene (PS).[18,20−23] Studies with poly(ethylene oxide) found results independent of probe size for probe diameters of 0.46−2 μm (all larger than the mesh size, polymer radius of gyration, and entanglement correlation length), suggesting the continuum limit is valid.[20,23] Further, studies of entangled PS, employing nanoparticles smaller than the polymer mesh size (as well as the radius of gyration and entanglement correlation length), measured anomalous diffusion rates much faster than those predicted by the Stokes−Einstein relation, demonstrating a breakdown of the continuum limit.[18,22] In contrast, recent findings for semidilute PEG suggest that the polymer radius of gyration, rather than the mesh size, is the threshold probe size for reaching the continuum limit.[21] For entangled polymers, several theoretical studies regarding the diffusion of spherical nanoparticles predict that the threshold probe radius, R, is the reptation tube diameter, d_T.[24−26] Recently, Yamamoto and Schweizer[26] used a statistical dynamics approach to build on these predictions and show that $R = d_T$ is not actually sufficient for the continuum limit; instead, the probe must be several times larger than the tube diameter, predicting a threshold criterion of $R \approx 5d_T$. Despite the widespread use of passive microrheology techniques to probe polymer systems,[16−18,21,27] this predicted crossover length scale has yet to be experimentally validated.

Received: July 31, 2013
Revised: January 21, 2014
Published: January 30, 2014

 © 2014 American Chemical Society dx.doi.org/10.1021/ma401615m | *Macromolecules* 2014, 47, 1181−1186

Compared to typical synthetic polymers, considerably larger length scales are encountered in biopolymer systems. For example, semiflexible actin filaments with persistence lengths of ~17 μm have been extensively studied by microrheology,[6,28−32] and evidence of noncontinuum effects (such as free diffusion and cage-hopping) has been reported for probe sizes similar to the mesh size.[9,15,30,33−36] However, the transition from the noncontinuum to the continuum regime, critical to understanding the microscopic nature of viscoelastic behavior in polymer systems, has not been characterized. The nature of such a transition also likely differs for more flexible biopolymers such as long DNA molecules in which the persistence length ($\approx$ 50 nm) is significantly smaller than the polymer length (~1−50 μm). In contrast to actin, relatively few microrheology studies of DNA have been carried out, and most have been in the semidilute or marginally entangled regime.[10,37−40] Probe sizes used in the reported studies were larger than the DNA mesh size and noncontinuum effects were not observed, indicating that the probes were sufficiently large to detect macroscopic properties. Thus, for entangled flexible polymers, the point of onset of noncontinuum effects has not been observed.

Here, we report studies of the transition from the continuum to noncontinuum regime in microrheology measurements with DNA, and the dependence on probe size and DNA length, including lengths longer than studied previously. We identify a threshold probe radius of ~$3d_T$ for entangled DNA, consistent with recent theoretical predictions.[26] For DNA, a model for flexible polymers in general, this threshold is significantly larger than the mesh size and typical probe sizes used in microrheology studies.

We used an active microrheology technique in which an optically trapped microsphere is driven sinusoidally at varying frequencies through DNA solutions while the resisting force is measured.[6,8] From these measurements we determined the storage modulus, $G'(\omega)$, which characterizes the elastic response, the loss modulus, $G''(\omega)$, which characterizes the viscous response, and the complex viscosity, $\eta^*(\omega)$, which is the ratio of complex modulus to frequency. We studied linear double-stranded DNA lengths of 11 kbp, 45 kbp, and 115 kbp at 1.0 mg/mL, which span the range from the unentangled to well-entangled regime with concentrations corresponding to $0.8c_e$, $2c_e$, and $4c_e$, respectively, where c_e is the critical concentration for entanglements (previously determined to be ~6× the polymer coil overlap concentration).[41] The mesh size for all three samples remains fixed (~100 nm), however the number of entanglements per molecule (n) increases with molecular length. Microspheres with radii of 1, 2.25, and 3 μm, all much larger than the DNA mesh size, were tested.

EXPERIMENTAL SECTION

Three double-stranded DNA constructs, an 11 kbp (3.7 μm) plasmid, a 45 kbp (15 μm) fosmid, and a 115 kbp (39 μm) bacterial artificial chromosome were prepared by replication of cloned constructs in *Escherichia coli*, followed by extraction and purification. One-cutter restriction enzymes, BamH1 (for 11 kbp), ApaI (45 kbp), and MluI (115 kbp), were used to convert the supercoiled constructs to linear form. These protocols have been thoroughly described previously.[42,43] For measurements, DNA solutions were prepared in aqueous buffer (10 mM Tris-HCl (pH 8), 1 mM EDTA, 10 mM NaCl) at a concentration of 1.0 mg/mL. Microspheres, with radii of 1, 2.25, and 3 μm (Polysciences), were coated with Alexa-Fluor-488 BSA (Invitrogen) to prevent nonspecific binding and to visualize the microspheres. Trace amounts of coated microspheres were mixed with the prepared DNA solutions and the solution was equilibrated for ~30 min prior to measurements.

A custom-built force-measuring optical trap, formed by a 1064 nm Nd:YAG DPSS laser (CrystaLaser) focused with a 60X 1.4 NA objective (Olympus), was used to capture individual microspheres within the sample chamber. The DNA solutions were displaced relative to the fixed trap using a piezoelectric nanopositioning stage (Mad City Laboratories) to apply a sinusoidal oscillation. A position-sensing detector (Pacific Silicon Sensors) measured the trapping laser deflection, which is proportional to the force acting on the trapped microsphere. The trap was calibrated using Stokes drag for a microsphere oscillating in water. The oscillation amplitude was chosen to be 0.52 μm as this was found to be sufficiently large to obtain a clear signal while being small enough that the response was not amplitude dependent (in the near-equilibrium regime of material response).

As depicted in Figure 1, force measurements for individual trials were each fit to a sine curve using the least-squares method. The resulting fit for each force trace and the recorded stage position are used to calculate the storage modulus, $G'(\omega) = [|F_{max}|/(|x_{stage}|6\pi R)]\cos(\Delta\varphi)$, loss modulus, $G''(\omega) = [|F_{max}|/(|x_{stage}|6\pi R)]\sin(\Delta\varphi)$, and complex viscosity, $\eta^*(\omega) = [(G'(\omega)/\omega)^2 + (G''(\omega)/\omega)^2]^{1/2}$, as described previously,[6] where $|F_{max}|$ is amplitude of measured force, $|x_{stage}|$ is stage amplitude, and $\Delta\varphi$ is phase difference between stage position and recorded force signal. Ten trials, each an average of 10 full oscillations, were completed for each frequency, with a new microsphere captured in a different region of the sample chamber for each trial. Average and standard deviation of $G'(\omega)$, $G''(\omega)$, and $\eta^*(\omega)$ for the 10 individual trials give the plotted values and error bars, respectively, for each frequency shown in Figures 2, 3, and 4.

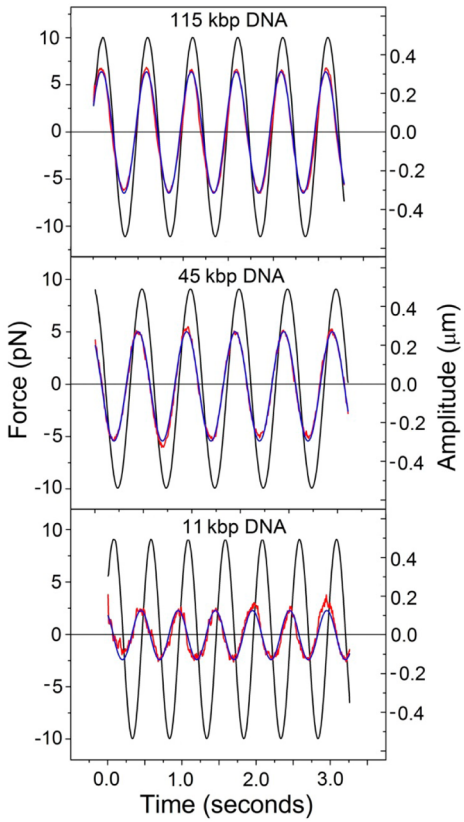

Figure 1. Measured force on a 1 μm radius microsphere (red, left axis) during ω = 12.57 rad s^{-1} stage oscillation (black, right axis). The blue curve is the fit to the raw force data (described in methods). The three panels show measurements in solutions of three different DNA lengths (specified at the top of each plot).

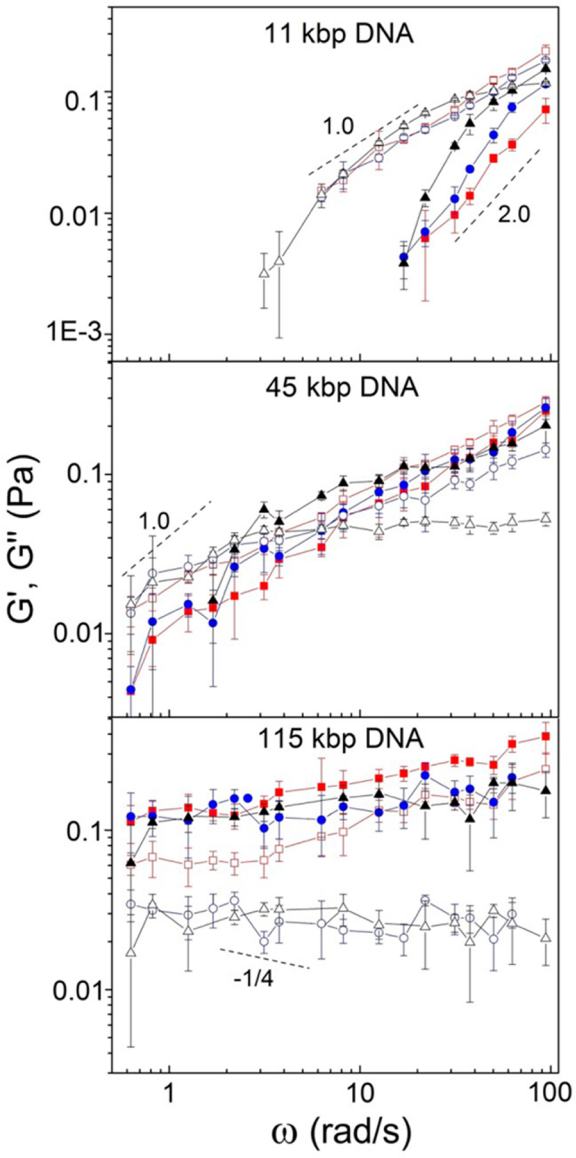

Figure 2. $G'(\omega)$ (closed symbols) and $G''(\omega)$ (open symbols) for 11, 45, and 115 kbp DNA measured with microspheres of radii: 1 μm (red squares), 2.25 μm (blue circles), and 3 μm (black triangles). Theoretically predicted scaling trends for the terminal regime ($G'(\omega) \sim \omega^2$, $G''(\omega) \sim \omega$) and the entangled regime ($G''(\omega) \sim \omega^{-1/4}$) are shown for comparison (dashed lines).

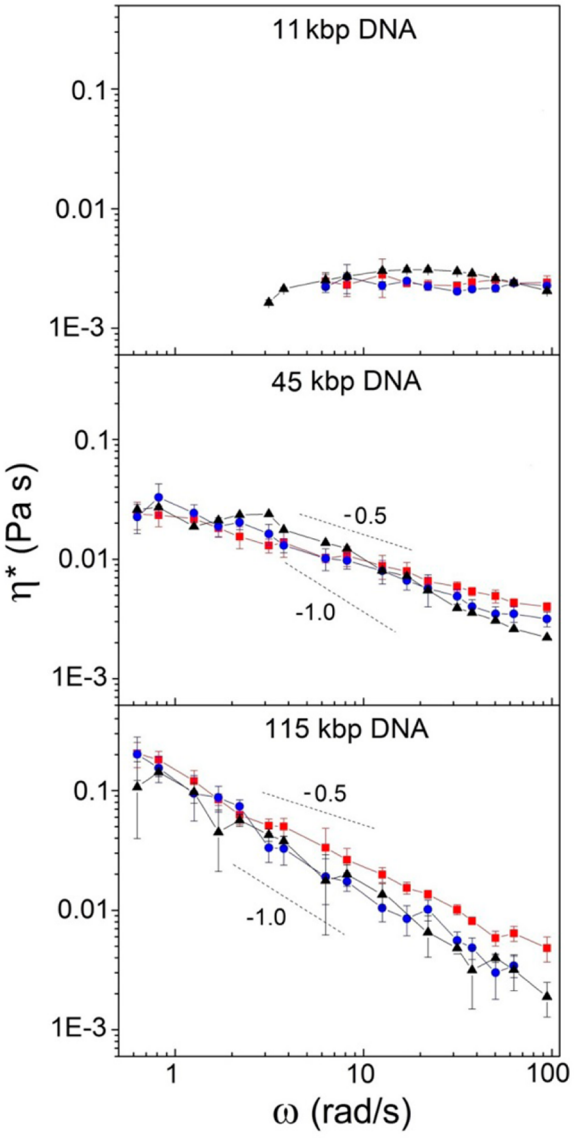

Figure 3. Complex viscosity, $\eta^*(\omega)$, measured with microspheres of radii 1 μm (red squares), 2.25 μm (blue circles), and 3 μm (black triangles) for each molecular length. Theoretically predicted scaling trends for semidilute ($\eta^*(\omega) \sim \omega^{-0.5}$) and fully entangled ($\eta^*(\omega) \sim \omega^{-1}$) solutions are shown for comparison.

RESULTS

For 11 kbp DNA ($0.8c_e$) microsphere size had a minimal effect compared with that for the two longer DNAs (Figure 2). $G'(\omega)$ displays similar scaling with frequency for all probe sizes with magnitudes increasing slightly with microsphere size. $G''(\omega)$ is essentially independent of microsphere size except for the highest frequency where a modest rollover is observed for 3 μm radius microspheres. Measurements are consistent with terminal relaxation regime scaling behavior, $G'(\omega) \sim \omega^2$ and $G''(\omega) \sim \omega$, predicted by tube models,[3] which indicates a low level of entanglements (as expected for $c < c_e$). Furthermore, the viscous response (G'') dominates over the measured frequency range, with the exception of the highest frequency for the 3 μm radius microspheres. The observed scaling of $G'(\omega)$ and $G''(\omega)$ for 11 kbp DNA is also consistent with that found in prior macrorheology measurements on calf-thymus DNA (polydisperse, ~13 kbp) at 1.0 mg/mL.[44,45] The measured complex viscosity, $\eta^*(\omega)$, also nearly probe size-independent

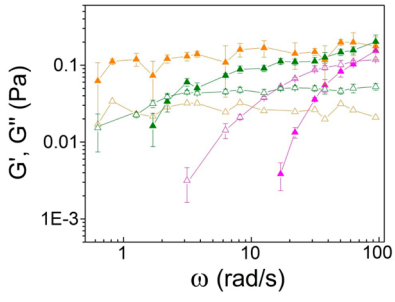

Figure 4. $G'(\omega)$ (closed symbols) and $G''(\omega)$ (open symbols) for 3 μm radius microspheres. Values for 11 kbp (magenta), 45 kbp (green), and 115 kbp (orange) DNA are shown.

dx.doi.org/10.1021/ma401615m | Macromolecules 2014, 47, 1181−1186

(Figure 3), is largely frequency-independent, further indication of the terminal relaxation regime.

A greater dependence on probe size was observed with 45 kbp DNA ($2c_e$), mainly for frequencies above ~2 rad s^{-1}. As entanglements play a larger role in the response at higher frequencies, this finding suggests that the effect of microsphere size is linked to polymer entanglements. Below ~2 rad s^{-1} both $G'(\omega)$ and $G''(\omega)$ scale as ω^x with $x < 1$, consistent with a transition from the terminal regime to entanglement-dominated regime.[3] In the well-entangled regime, reptation theory predicts that G' reaches a well-defined plateau, termed the plateau modulus,[3] G_N^0, and G'' scales as $\omega^{-1/4}$. The most conspicuous probe-size dependence is that G'' with 3 μm radius probes dramatically plateaus at high frequency whereas it continues to rise with the two smaller probes. Although we do not observe a decreasing trend, this plateau is consistent with a transition from $G''(\omega) \sim \omega$ to $G''(\omega) \sim \omega^{-1/4}$. For G', we do not observe a clear plateau for any probe size, but G' with the 3 μm probe rolls over toward an apparent high frequency plateau at lower frequencies than observed with the smaller probes. Observed scaling behavior for 3 μm radius probes is also similar to that observed in previous macrorheology measurements of 48.5 kbp DNA at 1.0 mg/mL.[19]

Measurements with 45 kbp DNA also show $G''(\omega) > G'(\omega)$ over the entire frequency range for 1 μm microspheres, in contrast to the larger microsphere data which both display a crossover frequency, ω_c, above which $G'(\omega) > G''(\omega)$. This crossover frequency is predicted to be inversely proportional to the disengagement time (τ_d) for entangled polymers, i.e. the time for an entangled polymer to reptate out of its confining tube.[1] Thus, only for $\omega > \omega_c$ is tube confinement (entanglements) predicted to dominate the response. Our data show polymer disengagement times of $\tau_d \leq 0.07$ s ($\omega_c \geq$ 95 rad s^{-1}), $\tau_d \approx 0.89$ s ($\omega_c \approx 7$ rad s^{-1}), and $\tau_d \approx 2.1$ s ($\omega_c \approx 3$ rad s^{-1}) for the 1, 2.25, and 3 μm radii microspheres, respectively. By estimating $\tau_d \approx 0.065$ s for the 1 μm radius spheres, the disengagement times exhibit power law scaling with bead radius of $\tau_d \sim R^{3.16\pm0.06}$ (Figure 5). This scaling of τ_d with microsphere size indicates that larger microspheres can more effectively probe entanglements, suggesting that the continuum limit has not yet been reached with the smaller probes.[25] This is also seen in the complex viscosity as the scaling exponent increases from ~−0.5 (predicted for the semidilute regime[19]) for 1 μm radius spheres to nearly −1, indicative of the entangled regime, for 3 μm spheres (Figure 3).

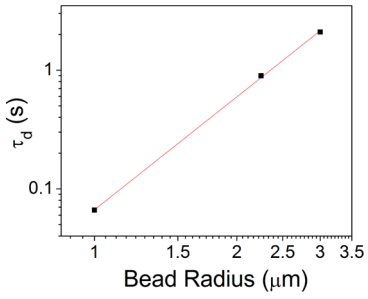

Figure 5. Polymer disengagement time (τ_d) vs bead radius (R) for 45 kbp DNA at 1.0 mg/mL. Disengagement times for each bead size (black squares) are determined from the measured crossover frequency for each bead size as described in the text. The data is fit to a power law $\tau_d \sim R^{3.16\pm0.06}$ (red line).

For the longest DNA (115 kbp, $4c_e$), $G'(\omega) > G''(\omega)$ across the entire frequency spectrum for all three microspheres (Figure 2), implying $\tau_d > 10$ s ($\omega_c < 0.63$ rad s^{-1}), which is consistent with our previous finding of $\tau_d \approx 30$ s for this system via single molecule force measurements.[46] This finding demonstrates that entanglements dominate the polymer response, as expected given $c \approx 4c_e$. However, while the measured viscoelastic moduli using 2.25 and 3 μm radius microspheres are nearly identical over the entire frequency range, the 1 μm radius microsphere data is distinctly different. For the two largest microspheres, $G'(\omega)$ is roughly constant over the entire frequency range, displaying a plateau modulus of $G_N^0 \approx 0.2$ Pa, while $G''(\omega)$ displays a decreasing trend consistent with the predicted $\omega^{-1/4}$ scaling for the entanglement-dominated regime.[3] In sharp contrast, $G'(\omega)$ and $G''(\omega)$ for 1 μm radius microspheres steadily increase with ω, indicating the probe is not behaving as if the well-entangled regime was reached. Further, the complex viscosity scales as $\eta^*(\omega) \sim \omega^{-1}$ for the two larger microspheres while the scaling exponent for 1 μm microspheres lies between −1 and −0.5 (Figure 3). These data indicate that for 115 kbp DNA only microspheres with radii larger than ~2 μm are fully sensitive to the molecular entanglements and thus have accessed the continuum limit, in contrast to the smaller microspheres which appear to be detecting fewer entanglements.

DISCUSSION

We have shown that microsphere size plays an important role in active microrheology measurements for entangled DNA, a model flexible polymer. We investigated the transition to noncontinuum behavior by conducting measurements with different probe sizes and DNA lengths, including longer DNA lengths than studied previously, and found a clear dependence on the degree of entanglement of the DNA. Our results suggest two distinct threshold probe sizes based on the level of polymer entanglement. For semidilute, unentangled DNA (11 kbp, $c < c_e$) the threshold probe radius is <1 μm, while for well-entangled DNA (115 kbp, $c \approx 4c_e$) it is ~2 μm.

One prior study observed a slight dependence of DNA microrheology results on microsphere size, but this was not found to be due to noncontinuum effects, but rather to a depletion-layer effect in which polymer concentration near the surface of the microspheres is altered.[38] While this effect can be important to consider, it becomes increasingly small for DNA concentrations above ~0.3 mg/mL and does not affect the frequency dependence of the moduli.[38,40,47] Therefore, this effect cannot explain the dramatic changes we observe in scaling behavior of the moduli with microsphere size with our longest DNA at 1 mg/mL.

Thus, how can we explain the value of a threshold probe size for entangled DNA? There are several relevant length scales associated with both the individual polymers and the polymer network that could play a role in the viscoelastic response. The length scales associated with the individual DNA molecules are: persistence length (~50 nm), molecular length (3.7, 15, and 39 μm), and radius of gyration (~0.3, 0.6, and 1.0 μm).[48] Length scales associated with the polymer network are: mesh size (~100 nm), tube diameter and polymer length between entanglements, l_e. l_e can be experimentally determined from the plateau modulus via the theoretically predicted relationship[1] $M_e = 4/5cRT/G_N^0$. For 3 μm microspheres, $G'(\omega)$ for all three DNA lengths approaches a value of ~0.2 Pa (Figure 4) giving $l_e \approx 5$ μm. As an aside, this finding verifies for the first time the

dx.doi.org/10.1021/ma401615m | Macromolecules 2014, 47, 1181−1186

predicted scaling $G_N^0 \sim M^0$ for entangled DNA.[49] The tube diameter is comparable to the spatial distance between entanglements, thus using our measured l_e and treating DNA as a random coil, we calculate a tube diameter of ~0.7 μm.

Several length scales listed above are on the order of the microsphere radii, including the molecular length. However, if the threshold length scale were the DNA length, then we should not observe agreement between 2.25 and 3 μm radius microspheres for the 115 kbp DNA as all microsphere sizes are smaller than the DNA length.

Motivated by theoretical predictions,[24−26] we can compare our threshold probe radius for well-entangled DNA (115 kbp, $n \approx 8$) to the tube diameter to find a criterion of $R \approx 3d_T$ for the continuum limit, which is closely aligned with the threshold size recently predicted by Yamamoto and Schweizer ($R \approx 5d_T$) for probe diffusion in typical entangled synthetic polymer melts.[24−26] This previously unvalidated threshold is demonstrated with 115 kbp DNA as we see microsphere-size independence only above $R \approx 2$ μm. Further, the measured scaling of G' and G'' with frequency for both the 2.25 and 3 μm radius microspheres ($\geq 3d_T$) is consistent with tube theory predictions for well-entangled polymers, in sharp contrast to the smaller 1 μm radius ($\sim 1.4d_T$) microspheres. We note that our criterion is actually slightly smaller than that predicted by Yamamoto and Schweizer which most likely stems from the different techniques addressed (passive probe diffusion vs actively driven probes) as well as the different systems investigated (synthetic polymer melts vs biopolymer solutions). Given these differences, the agreement between the theoretical predictions of Yamamoto and Schweizer and our experimental results lends credence to the universality of both results.

For 45 kbp DNA ($c \approx 2c_e$, $n \approx 3$), this threshold is not apparent as data for all three microsphere sizes differs. This is most likely due to the fact that 45 kbp DNA is only marginally entangled with ~3 entanglements per molecule. In fact, the predicted threshold of $R \approx 5d_T$ is only valid for well-entangled polymers with the criterion $n > 4$.[26] We can understand the probe size dependence for the 45 kbp DNA by analogy to cage-hopping, where probes diffusing through entanglements can exhibit increased diffusion by hopping to new entanglement cages, thereby momentarily avoiding entanglement constraints.[18,25] Similarly, if there are only a few entanglements in the vicinity of the probe, local fluctuations could momentarily release the probe from these constraints. This noncontinuum effect should become more significant as the probe size decreases. Our finding that the measured polymer disengagement time scales roughly as the volume of the probe ($\tau_d \sim R^{3.16\pm0.06}$) for the 45-kbp DNA (Figure 5) supports this interpretation and is in agreement with recent theoretical studies that suggest that the rate of cage-hopping decreases with probe size.[25]

Finally, for the semidilute, unentangled case (11 kbp, $n < 1$), our findings suggest agreement with recent theoretical studies that predict the threshold size for unentangled polymers is the radius of gyration.[26] Here, all probe sizes are larger than the radius of gyration (~0.3 μm for 11 kbp DNA), and yield similar results, with scaling of G' and G'' in good agreement with theoretical expectations and prior macrorheology studies.[1,3,44,45] We note that as all microsphere sizes are also larger than the mesh size, this could also be an important length scale for unentangled or weakly entangled polymers; however, distinguishing between the mesh size and the radius of gyration does not serve a practical purpose as both length scales are smaller than microsphere sizes used in most microrheology experiments.

We also note that throughout this discussion we have focused on the consequences of a probe being too small, however in microrheology if a probe becomes too large, this could also lead to systematic errors in the measured response. For instance, in our experimental design the microspheres and polymer solution are in a sample chamber with a thickness of ~100 μm. If the trapped probe approaches either surface during oscillation, surface interactions will influence the measured response and the optical trap characteristics. Thus, we would suggest that a probe not be larger than ~10 μm to eliminate any unwanted experimental artifacts; however, testing this limit is left open for future studies.

■ CONCLUSION

We have used active microrheology measurements with optical tweezers, employing microspheres of varying radii, to characterize the effect of probe size on measured linear viscoelastic properties of entangled DNA (a model flexible polymer) of varying lengths and degrees of entanglement. We have found that for unentangled solutions, where the molecular length is less than the length between entanglements, the storage and loss moduli reveal only a weak dependence on microsphere size, provided the microsphere radius is larger than the radius of gyration. However, the microsphere radius becomes more relevant as the number of entanglements per molecule increases (i.e., the length of the molecule becomes significantly larger than l_e). We propose that for well-entangled flexible polymers, microrheology measurements of linear viscoelastic properties only become microsphere size independent for microspheres with radii larger than ~3 times the tube diameter. Given that this threshold is significantly larger than the mesh size for flexible polymers (e.g., ~2 μm vs 100 nm for 115 kbp DNA at 1 mg/mL), and larger than typical microsphere sizes used in microrheology experiments, this finding must be carefully considered. Considering the current widespread use of microrheology to characterize biopolymer systems, this finding is important to understanding the complex relationship between stress and strain in these materials at the molecular level.

■ AUTHOR INFORMATION

Corresponding Author

*(R.M.R.-A.) E-mail: randerson@sandiego.edu.

Notes

The authors declare no competing financial interest.

■ ACKNOWLEDGMENTS

We thank S. Church, and I. Masongsong for assistance with sample preparation. R.M.R-A acknowledges the Research Corporation and AFOSR YIP (Grant No. FA9550-12-1-0315) for funding this research.

■ REFERENCES

(1) Doi, M.; Edwards, S. F. *The theory of polymer dynamics*; Oxford University Press: New York, 1986.

(2) Larson, R. G. *The structure and rheology of complex fluids*; Oxford University Press: New York, 1999.

(3) McLeish, T. C. B. *Adv. Phys.* **2002**, *51* (6), 1379−1527.

(4) Witten, T. A.; Pincus, P. A., *Structured fluids: polymers, colloids, surfactants*. Oxford University Press on Demand: New York, 2004.

(5) Zaner, K. S.; Valberg, P. A. *J. Cell Biol.* **1989**, *109* (5), 2233−43.

(6) Ziemann, F.; Radler, J.; Sackmann, E. *Biophys. J.* **1994**, *66* (6), 2210−6.
(7) Mason, T. G.; Weitz, D. *Phys. Rev. Lett.* **1995**, *74* (7), 1250−1253.
(8) Valentine, M.; Dewalt, L.; Ou-Yang, H. *J. Phys.: Condens. Matter* **1996**, *8* (47), 9477.
(9) Gittes, F.; Schnurr, B.; Olmsted, P. D.; MacKintosh, F. C.; Schmidt, C. F. *Phys. Rev. Lett.* **1997**, *79* (17), 3286−3289.
(10) Mason, T. G.; Ganesan, K.; vanZanten, J. H.; Wirtz, D.; Kuo, S. C. *Phys. Rev. Lett.* **1997**, *79* (17), 3282−3285.
(11) MacKintosh, F.; Schmidt, C. *Curr. Opin. Colloid Interface Sci.* **1999**, *4* (4), 300−307.
(12) Gardel, M. L.; Valentine, M. T.; Weitz, D. A. Microrheology. In *Microscale diagnostic techniques*: Springer: Berlin, 2005; pp 1−49.
(13) Savin, T.; Doyle, P. S. *Biophys. J.* **2005**, *88* (1), 623−638.
(14) Graham, R. S.; McLeish, T. C. B. *J Non-Newton Fluid* **2008**, *150* (1), 11−18.
(15) Squires, T. M.; Mason, T. G. *Annu. Rev. Fluid Mech.* **2010**, *42*, 413−438.
(16) Köster, S.; Lin, Y.-C.; Herrmann, H.; Weitz, D. A. *Soft Matter* **2010**, *6* (9), 1910−1914.
(17) Kotlarchyk, M.; Botvinick, E.; Putnam, A. *J. Phys.: Condensed Matter* **2010**, *22* (19), 194121.
(18) Guo, H.; Bourret, G.; Lennox, R. B.; Sutton, M.; Harden, J. L.; Leheny, R. L. *Phys. Rev. Lett.* **2012**, *109* (5), 055901.
(19) Teixeira, R. E.; Dambal, A. K.; Richter, D. H.; Shaqfeh, E. S. G. *Macromolecules* **2007**, *40* (9), 3514−3514.
(20) Dasgupta, B. R.; Tee, S. Y.; Crocker, J. C.; Frisken, B. J.; Weitz, D. A. *Phys. Rev. E* **2002**, *65*, 051505.
(21) Kohli, I.; Mukhopadhyay, A. *Macromolecules* **2012**, *45* (15), 6143−6149.
(22) Tuteja, A.; Mackay, M. E.; Narayanan, S.; Asokan, S.; Wong, M. S. *Nano Lett.* **2007**, *7* (5), 1276−81.
(23) van Zanten, J. H.; Amin, S.; Abdala, A. A. *Macromolecules* **2004**, *37* (10), 3874−3880.
(24) Wyart, F. B.; De Gennes, P. *Eur. Phys. J. E* **2000**, *1* (1), 93−97.
(25) Cai, L.-H.; Panyukov, S.; Rubinstein, M. *Macromolecules* **2011**, *44* (19), 7853−7863.
(26) Yamamoto, U.; Schweizer, K. S. *J. Chem. Phys.* **2011**, *135* (22), 224902−224902−16.
(27) Lu, Q.; Solomon, M. J. *Phys. Rev. E* **2002**, *66* (6), 061504.
(28) Maggs, A. C. *Phys. Rev. E* **1998**, *57* (2), 2091−2094.
(29) Xu, J. Y.; Palmer, A.; Wirtz, D. *Macromolecules* **1998**, *31* (19), 6486−6492.
(30) Schmidt, F. G.; Hinner, B.; Sackmann, E. *Phys. Rev. E* **2000**, *61* (5), 5646−5653.
(31) Gardel, M. L.; Valentine, M. T.; Crocker, J. C.; Bausch, A. R.; Weitz, D. A. *Phys. Rev. Lett.* **2003**, *91* (15), 158302.
(32) Liu, J.; Gardel, M. L.; Kroy, K.; Frey, E.; Hoffman, B. D.; Crocker, J. C.; Bausch, A. R.; Weitz, D. A. *Phys. Rev. Lett.* **2006**, *96* (11), 118104.
(33) Schnurr, B.; Gittes, F.; MacKintosh, F. C.; Schmidt, C. F. *Macromolecules* **1997**, *30* (25), 7781−7792.
(34) McGrath, J. L.; Hartwig, J. H.; Kuo, S. C. *Biophys. J.* **2000**, *79* (6), 3258−3266.
(35) Valentine, M. T.; Perlman, Z. E.; Gardel, M. L.; Shin, J. H.; Matsudaira, P.; Mitchison, T. J.; Weitz, D. A. *Biophys. J.* **2004**, *86* (6), 4004−4014.
(36) Wong, I. Y.; Gardel, M. L.; Reichman, D. R.; Weeks, E. R.; Valentine, M. T.; Bausch, A. R.; Weitz, D. A. *Phys. Rev. Lett.* **2004**, *92* (17), 178101.
(37) Goodman, A.; Tseng, Y.; Wirtz, D. *J. Mol. Biol.* **2002**, *323* (2), 199−215.
(38) Chen, D. T.; Weeks, E. R.; Crocker, J. C.; Islam, M. F.; Verma, R.; Gruber, J.; Levine, A. J.; Lubensky, T. C.; Yodh, A. G. *Phys. Rev. Lett.* **2003**, *90* (10), 108301.
(39) Gutsche, C.; Kremer, F.; Kruger, M.; Rauscher, M.; Weeber, R.; Harting, J. *J. Chem. Phys.* **2008**, *129* (8), 084902.
(40) Zhu, X. Y.; Kundukad, B.; van der Maarel, J. R. C. *J. Chem. Phys.* **2008**, *129* (18), 185103.
(41) Robertson, R. M.; Smith, D. E. *Macromolecules* **2007**, *40* (9), 3373−3377.
(42) Laib, S.; Robertson, R. M.; Smith, D. E. *Macromolecules* **2006**, *39* (12), 4115−4119.
(43) Chapman, C. D.; Shanbhag, S.; Smith, D. E.; Robertson-Anderson, R. M. *Soft Matter* **2012**, *8* (35), 9177−9182.
(44) Mason, T. G.; Dhople, A.; Wirtz, D. *Macromolecules* **1998**, *31* (11), 3600−3603.
(45) Bandyopadhyay, R.; Sood, A. K. *Pramana-J. Phys.* **2002**, *58* (4), 685−694.
(46) Robertson, R. M.; Smith, D. E. *Phys. Rev. Lett.* **2007**, *99* (12), 126001.
(47) Levine, A. J.; Lubensky, T. C. *Phys Rev E* **2001**, *63* (4), 041510.
(48) Robertson, R. M.; Laib, S.; Smith, D. E. *Proc. Natl. Acad. Sci. U.S.A.* **2006**, *103* (19), 7310−7314.
(49) Graessley, W.; Edwards, S. *Polymer* **1981**, *22* (10), 1329−1334.